HYPERFINE STRUCTURE IN THE MICROWAVE SPECTRUM OF WATER

II. EFFECTS OF MAGNETIC INTERACTIONS

By D. W. POSENER*

[*Manuscript received March* 10, 1960]

Summary

Further analysis of the hyperfine structure appearing in the observed microwave spectra of HDO and D_2O, taking into account nuclear quadrupole and magnetic dipole interactions, leads to a complete determination of the electric field gradient tensor at the hydrogen nuclei in the water molecule, giving a value along the bond direction of $(+1\cdot59\pm0\cdot04)\times10^{15}$ e.s.u.

Parameters describing magnetic effects in the observed spectra have also been obtained.

I. INTRODUCTION

The partially resolved microwave spectra of the $2_{20}\leftarrow2_{21}$ transition of HDO at 10,278 Mc/s and of the $3_{13}\leftarrow2_{20}$ line of D_2O at 10,919 Mc/s have been previously described (Posener 1957, hereafter referred to as I) and the results for D_2O analysed on the assumption that only nuclear quadrupole coupling effects contributed significantly to the observed hyperfine structure. It was there concluded that the quadrupole coupling constant of the deuteron in the direction of the OD bond was $(eqQ)_{OD}=+353\pm4$ kc/s, and that it was not possible to account for the HDO spectrum if only the nuclear quadrupolar interaction were taken into account.

Improved agreement between calculated and observed spectra has now been obtained by including effects due to magnetic interactions occurring within the molecules ; it will be shown that neglect of these effects in the previous analysis of D_2O introduced a systematic error of some 10 per cent. in the estimation of $(eqQ)_{OD}$.

II. THEORY

(*a*) *Calculation of Transition Frequencies*

Hyperfine structure in the rotational spectra of HDO and D_2O arises from interaction of the magnetic dipole and nuclear quadrupole moments of the hydrogen and deuterium nuclei with the various electric and magnetic fields occurring in the rotating molecules. The generalized theory of such interactions has been published (Posener 1958, hereafter referred to as II), and our notation will follow this work unless otherwise stated.

* Division of Electrotechnology, C.S.I.R.O., University Grounds, Chippendale, N.S.W.

TABLE 1

ENERGY MATRIX FOR HDO, $J=2$

F_1,F	1,1/2	1,3/2	2,3/2	2,5/2	3,5/2	3,7/2
1,1/2	$\frac{1}{6}(\alpha(Q)+\alpha(S))$ $+\frac{1}{2}\left(c(\mathrm{D})+\frac{1}{2}c(\mathrm{H})\right)$					
1,3/2		$\frac{1}{6}\left(\alpha(Q)-\frac{1}{2}\alpha(S)\right)$ $+\frac{1}{2}\left(c(\mathrm{D})-\frac{1}{4}c(\mathrm{H})\right)$	$\frac{1}{8}c(\mathrm{H})$			
2,3/2		$\frac{1}{8}c(\mathrm{H})$	$-\frac{1}{6}\left(\alpha(Q)-\frac{1}{2}\alpha(S)\right)$ $+\frac{1}{6}\left(c(\mathrm{D})+\frac{5}{4}c(\mathrm{H})\right)$			
2,5/2				$-\frac{1}{6}\left(\alpha(Q)+\frac{1}{3}\alpha(S)\right)$ $+\frac{1}{6}\left(c(\mathrm{D})-\frac{5}{6}c(\mathrm{H})\right)$	$-\frac{14^{\frac{1}{2}}}{36}\left(\frac{5}{7}\alpha(S)-c(H)\right)$	
3,5/2				$-\frac{14^{\frac{1}{2}}}{36}\left(\frac{5}{7}\alpha(S)-c(\mathrm{H})\right)$	$\frac{1}{21}\left(\alpha(Q)-\frac{4}{3}\alpha(S)\right)$ $-\frac{1}{3}\left(c(\mathrm{D})-\frac{2}{3}c(\mathrm{H})\right)$	
3,7/2						$\frac{1}{21}(\alpha(\mathrm{Q})+\alpha(\mathrm{S}))$ $-\frac{1}{3}\left(c(\mathrm{D})+\frac{1}{2}c(\mathrm{H})\right)$

TABLE 2

ENERGY MATRIX FOR D_2O, $J=2$

I,F	2,0	2,1	0,2	2,2	2,3	2,4
2,0	$\frac{1}{3}(\alpha(Q)+\alpha(S))+c(\mathrm{D})$					
2,1		$\frac{1}{6}(\alpha(Q)+\alpha(S))+\frac{5}{6}c(\mathrm{D})$				
0,2			0	$\frac{1}{63^{\frac{1}{2}}}(2\alpha(Q)-\alpha(S))$		
2,2			$\frac{1}{63^{\frac{1}{2}}}(2\alpha(Q)-\alpha(S))$	$-\frac{1}{14}(\alpha(Q)+\alpha(S))+\frac{1}{2}c(\mathrm{D})$		
2,3					$-\frac{4}{21}(\alpha(Q)+\alpha(S))$	
2,4						$\frac{2}{21}(\alpha(Q)+\alpha(S))-\frac{2}{3}c(\mathrm{D})$

TABLE 3

ENERGY MATRIX FOR D_2O, $J=3$

I,F	2,1	2,2	0,3	2,3	2,4	2,5
2,1	$\frac{2}{15}(\alpha(Q)+\alpha(S))+\frac{2}{3}c(\mathrm{D})$					
2,2		$\frac{1}{30}(\alpha(Q)+\alpha(S))+\frac{1}{2}c(\mathrm{D})$				
0,3			0	$\frac{1}{270^{\frac{1}{2}}}(2\alpha(Q)-\alpha(S))$		
2,3			$\frac{1}{270^{\frac{1}{2}}}(2\alpha(Q)-\alpha(S))$	$-\frac{11}{180}(\alpha(Q)+\alpha(S))+\frac{1}{4}c(D)$		
2,4					$-\frac{1}{12}(\alpha(Q)+\alpha(S))-\frac{1}{12}c(\mathrm{D})$	
2,5						$\frac{1}{18}(\alpha(Q)+\alpha(S))-\frac{1}{2}c(\mathrm{D})$

Choosing for HDO the $I_1JF_1I_2FK$ representation, in which $\mathbf{I}_1$ is the spin of the deuterium nucleus ($I_1=1$) and $\mathbf{I}_2$ the spin of the nucleus of hydrogen ($I_2=\frac{1}{2}$), the matrix elements of the hyperfine structure part of the Hamiltonian may be obtained directly from II, equation (**58**), noting that $\alpha^{(2)}_{J,\tau}=0$, since the hydrogen nucleus has no quadrupole moment. For conciseness we will replace $\alpha^{(1)}_{J,\tau}$, $\alpha^{(S)}_{J,\tau}$, $c^{(1)}_{J,\tau}$, and $c^{(2)}_{J,\tau}$ by $\alpha^{(Q)}$, $\alpha^{(S)}$, $c^{(D)}$, and $c^{(H)}$ respectively, with the rotational state energy dependence implied if not indicated by subscripts. Also, we use the J_{K_a,K_c} subscript notation for rotational states rather than J_τ. Then, with $J=2$, the hyperfine structure energy matrix for HDO becomes as shown in Table 1, to the approximations discussed in II.

More appropriate for D_2O is the I_2I_1IJFK representation, in which $\mathbf{I}_1$ and $\mathbf{I}_2$ are the spins of the two deuterium nuclei ($I_1=I_2=1$). Allowing for the molecular symmetry the matrix elements for $J=2$ and $J=3$, as given by II, equation (**53**), are as shown in Tables 2 and 3.

The magnetic dipole-dipole interaction terms $\alpha^{(S)}$ occurring in the energy matrices may be computed as constants from II, equation (**54**), using equilibrium internuclear distances for sufficient accuracy since the zero-point vibrations will not significantly affect the results. We have used (Herzberg 1945, p. 489): $r_e=0\cdot9584\times10^{-8}$ cm, and $\angle\mathrm{HOH}=104°\ 27'$. With the $\langle J_g^2\rangle$'s calculated from rotational constants given elsewhere (Posener 1953), the dipole-dipole terms become as shown in Table 4.*

TABLE 4

MAGNETIC DIPOLE-DIPOLE INTERACTION CONSTANTS

HDO		D_2O	
$\alpha^{(S)}_{2_{20}}$	$-25\cdot8$ kc/s	$\alpha^{(S)}_{3_{13}}$	$7\cdot3$ kc/s
$\alpha^{(S)}_{2_{21}}$	$-25\cdot6$ kc/s	$\alpha^{(S)}_{2_{20}}$	$-4\cdot8$ kc/s

When a diagonalizing transformation $\mathbf{R}$ is applied to these matrices $\mathbf{H}$, the resulting diagonal matrices $\tilde{\mathbf{R}}\mathbf{H}\mathbf{R}$ give the energy splittings of the rotational levels, and thus the frequency shifts from the "unperturbed" line centres ν_0 can be obtained. (The tilde denotes the matrix transpose. In the sequel an unprimed matrix will refer to the lower rotational state, a primed matrix to the upper state.)

Although the hyperfine interactions result in considerable mixing of the "unperturbed" states, so that F_1 (in HDO) and I (in D_2O) are no longer good quantum numbers, it is convenient to retain them as labels for a description of the actual energy levels.

* In II, p. 2, it was incorrectly stated that nuclei have magnetic moments $g_k\mu_N$; this should read $g_k\mu_NI_k$. Because of this error the nuclear g-factor for hydrogen was taken as half its correct value of $g_H=+5\cdot585340$ and the calculations on HDO were actually carried through with values of $\alpha^{(S)}$ half those shown in Table 4. As discussed below (Section IV (c)) it is not now considered that a recalculation is warranted.

(*b*) *Calculation of Relative Intensities*

The intensity of a transition $a' \leftarrow a$ is proportional to $|(a \mid \boldsymbol{\mu} \mid a')|^2$, where $(a \mid \boldsymbol{\mu} \mid a')$ is the dipole moment matrix ; the total intensity A of a line is the sum of its components, which in the present case arise only from the degeneracy in M_F. If $\boldsymbol{\mu}$ stands for the dipole moment matrix in a representation in which the energy is not diagonal, then in the notation of the previous section

$$(a \mid \boldsymbol{\mu} \mid a') = \tilde{\mathbf{R}}\boldsymbol{\mu}\mathbf{R}', \quad \ldots\ldots\ldots\ldots\ldots\ldots \quad (1)$$

and so

$$A = \sum_{M_F, M_F'} | \tilde{\mathbf{R}}\boldsymbol{\mu}\mathbf{R}' |^2. \quad \ldots\ldots\ldots\ldots \quad (2)$$

For the hyperfine structure in HDO and D_2O, in the non-diagonal representations $I_1JF_1I_2FK$ and I_2I_1IJFK respectively, we can use II, equation (**12**), to factor out the dependence on F_1 and F (or I and F) because the dipole moment and the nuclear spin operators commute. Then, omitting irrelevant quantum numbers, we get for the elements of $\boldsymbol{\mu}$,

$$\begin{aligned} \boldsymbol{\mu}(\mathrm{HDO}) &= (JKM_F \vdots \boldsymbol{\mu} \vdots J'K'M_F')(JF_1 \mid J'F_1')(F_1F \mid F_1'F'), \\ \boldsymbol{\mu}(\mathrm{D_2O}) &= (JKM_F \vdots \boldsymbol{\mu} \vdots J'K'M_F')(IJF \mid IJ'F'). \quad \ldots\ldots\ldots\ldots \quad (3) \end{aligned}$$

The transformation indicated in (**1**) is diagonal in F and M_F, so its application to the expressions in (**3**) does not affect the first factors on the right of these equations. If the now transformed dipole moment matrix is put into (**2**) and the summation over M_F, M_F', and the polarizations is carried out (Condon and Shortly 1953, equation **7**[**4**]**5**), and if we then omit factors irrelevant to the hyperfine structure problem, the result can be written as

$$\begin{aligned} A(\mathrm{HDO}) &= | \tilde{\mathbf{R}} B(\mathrm{HDO}) \mathbf{R}' |^2, \\ A(\mathrm{D_2O}) &= | \tilde{\mathbf{R}} B(\mathrm{D_2O}) \mathbf{R}' |^2, \quad \ldots\ldots\ldots\ldots\ldots\ldots \quad (4) \end{aligned}$$

where

$$\begin{aligned} B(\mathrm{HDO}) &= [(2F+1)\Xi(F,F')]^{\frac{1}{2}}(JF_1 \mid J'F_1')(F_1F \mid F_1'F'), \\ B(\mathrm{D_2O}) &= [(2F+1)\Xi(F,F')]^{\frac{1}{2}}(IJF \mid IJ'F'). \quad \ldots\ldots\ldots\ldots \quad (5) \end{aligned}$$

The matrix elements $B(\mathrm{HDO})$ and $B(\mathrm{D_2O})$ are shown in Tables 5 and 6 respectively.

III. Analysis of the Observations

The preceding theory shows that it is possible to calculate the hyperfine structure frequencies and relative intensities for the two molecules in terms of the fairly small number of variables appearing in the Hamiltonian. However, because of the small magnitude of the interactions involved, the observed transitions lie close together and the experimental technique could not completely separate them. As shown in I, only a general profile of the intensity as a function of frequency was measured, with occasionally a prominent peak more completely resolved. Nevertheless, a considerable amount of information is contained in such measurements, so the problem became one of calculating line profiles and

adjusting the variables until adequate agreement with experiment was obtained. Most of the large amount of numerical work required to do this was carried out with the aid of the digital computer SILLIAC* in about 30 hours of computing; about two-thirds of this time was, however, employed on program development and exploratory calculations.

TABLE 5
THE MATRIX B(HDO) FOR $J=2\leftarrow2$

		2_{20}					
	F_1',F' / F_1,F	1,1/2	1,3/2	2,3/2	2,5/2	3,5/2	3,7/2
2_{21}	1,1/2	$6^{\frac{1}{2}}$	$-3^{\frac{1}{2}}$	$-3^{\frac{1}{2}}$			
	1,3/2	$-3^{\frac{1}{2}}$	$15^{\frac{1}{2}}$	$-(3/5)^{\frac{1}{2}}$	$-(27/5)^{\frac{1}{2}}$		
	2,3/2	$-3^{\frac{1}{2}}$	$-(3/5)^{\frac{1}{2}}$	$15^{\frac{1}{2}}$	$-(5/3)^{\frac{1}{2}}$	$-(56/15)^{\frac{1}{2}}$	
	2,5/2		$-(27/5)^{\frac{1}{2}}$	$-(5/3)^{\frac{1}{2}}$	$(70/3)^{\frac{1}{2}}$	$-2/15^{\frac{1}{2}}$	$-4/3^{\frac{1}{2}}$
	3,5/2			$-(56/15)^{\frac{1}{2}}$	$-2/15^{\frac{1}{2}}$	$(640/21)^{\frac{1}{2}}$	$-(32/21)^{\frac{1}{2}}$
	3,7/2				$-4/3^{\frac{1}{2}}$	$-(32/21)^{\frac{1}{2}}$	$(288/7)^{\frac{1}{2}}$

TABLE 6
THE MATRIX $B(D_2O)$ FOR $J=3\leftarrow2$

		3_{13}					
	I',F' / I,F	2,1	2,2	0,3	2,3	2,4	2,5
2_{20}	2,0	$21^{\frac{1}{2}}$					
	2,1	$21^{\frac{1}{2}}$	$42^{\frac{1}{2}}$				
	0,2			$105^{\frac{1}{2}}$			
	2,2	$-3^{\frac{1}{2}}$	$30^{\frac{1}{2}}$		$72^{\frac{1}{2}}$		
	2,3		$-3^{\frac{1}{2}}$		$(63/2)^{\frac{1}{2}}$	$15/2^{\frac{1}{2}}$	
	2,4				$-(3/2)^{\frac{1}{2}}$	$(45/2)^{\frac{1}{2}}$	$165^{\frac{1}{2}}$

* Adolph Basser Computing Laboratory, University of Sydney.

At first a Lorentz profile was used to calculate the amount each transition contributed to the intensity profile at a given frequency ; however, the Doppler contribution to the broadening was of like magnitude, and later calculations took this into account with subsequent improvement in the agreement between calculated and observed profiles. A numerical integration method was used for computation of this combined effect (Posener 1959).

It was initially hoped that the whole problem could be solved automatically on the computer ; a program was written to calculate the line profiles for a given set of initial variables, and a " steepest descent " method used to minimize the sum of squares of residuals between observed and calculated ordinates. As an initial approximation, values corresponding to the results of I were used, i.e. $(eqQ)_{OD}=353$ kc/s and all the $c^{(k)}$ taken as zero. Although it was possible to decrease the sum of squares, the results did not significantly improve agreement with the observed line profiles because the initial approximation was poor and the calculation became trapped in various shallow minima which abound in the multidimensional surface. Similar difficulties arose when other initial approximations were used.

It became clear that, because of the relatively poor initial approximation, the minimization of the sum of squares of the residuals was alone not a sufficiently powerful criterion for automatic solution of the problem. This was then broken into parts, an approach which proved successful. Firstly, a set of $\alpha^{(Q)}$ and $c^{(k)}$ was obtained to fit the HDO profile ; secondly, a similar set was found for D_2O ; finally, these were combined.

In order to fit the HDO spectrum alone, $\alpha^{(Q)}=434$ kc/s, corresponding to $(eqQ)_{OD}=353$ kc/s, was taken as approximately correct, and trial profiles computed for $c^{(D)}=-500(50)+500$ kc/s, $c^{(H)}=-1000(50)+1000$ kc/s, a range which ought to cover all reasonably expected values of these parameters. At this stage no distinction was made between parameter values for the upper and lower states, for which the difference should be quite small. It was found that general agreement with the observed profile occurred only in one very restricted area of this net, and by examining this region with smaller mesh sizes a good fit was obtained for $c^{(D)}\sim+10$ kc/s, $c^{(H)}\sim+240$ kc/s.

At this point empirical refinements, such as adjustment of the line " centre " ν_0 and of the line-width parameters $\Delta\nu_L$ (Lorentz half half-width) and $\Delta\nu_D$ (Doppler half half-width) were carried out ; subsequently it was found that use of the Doppler-Lorentz profile did not significantly affect the fit in so far as the frequencies of transitions were concerned, although the overall agreement was much better. For $\Delta\nu_D$ the value 12·0 kc/s (calculated for the experimental conditions) gave satisfactory results, and trial variations of several kc/s in this value (keeping the total line width constant) did not appear to change the results significantly.

Having now obtained something which looked like the observed profile, i.e. a good initial approximation, more refined techniques could be applied. By examining the individual transitions and, where desirable, shifting them one at a time independently so as to synthesize a profile agreeing somewhat better with the measured one, it became possible to " estimate " the frequencies of the

unresolved transitions with some accuracy. Following this, the effects of small changes in the parameters $\alpha^{(Q)}$ and $c^{(k)}$ on the frequencies of these transitions gave a set of linear equations to which a least squares fit could be made in order to further improve the parameters. The whole process was repeated as necessary until significant improvement ceased to be obtained.

TABLE 7

HDO $2_{20}\leftarrow 2_{21}$ HYPERFINE TRANSITION FREQUENCIES AND RELATIVE INTENSITIES*

		2_{20}					
	F_1',F' / F_1,F	1,1/2	1,3/2	2,3/2	2,5/2	3,5/2	3,7/2
2_{21}	1,1/2	—	**172±2**	—			
		244·4	168·3	76·9			
		14·58	*12·17*	*2·42*			
	1,3/2	**320±2**	—	—	**80±1**	—	
		322·3	246·2	154·8	80·3	265·1	
		12·48	*27·05*	*0·48*	*15·27*	*3·04*	
	2,3/2	—	—	—	—	**354±2**	
		409·9	333·8	242·4	167·9	352·6	
		2·10	*1·11*	*47·19*	*0·00*	*7·93*	
	2,5/2		**411±1**	—	—	—	**331±2**
			410·2	318·8	244·3	429·0	329·7
			15·20	*0·03*	*60·63*	*0·91*	*10·74*
	3,5/2		—	**135±2**	—	—	**144±2**
			225·6	134·2	59·7	244·5	145·2
			2·80	*8·23*	*0·81*	*69·74*	*5·93*
	3,7/2				**165±2**	**350±2**	—
					163·2	348·0	248·6
					10·79	*5·88*	*100·00*

* The first line of each row shows the estimated frequency (bold type) and the second line shows the frequency calculated from the best HDO parameters (column (*a*) of Table 9). All frequencies are in kc/s above 10,278·000 Mc/s. The last line of each row gives the relative intensities (italics).

Estimated (using this word in the sense described above) transition frequencies for HDO are shown in Table 7,* together with the frequencies calculated from the best parameters (listed in Table 9). The corresponding profiles are shown in Figure 1, and, to a larger scale, in Figure 2. The latter may be compared with the spectrogram of Figure 3, which shows the corresponding part of the HDO spectrum at higher gain and was obtained at the same time as the experimental results reported in I.

* All error limits quoted for the present work are r.m.s. errors.

In the case of D_2O, the initial approximation of pure quadrupolar coupling already gave a good fit with the positions of the major transitions approximately known (see I), and again corresponding to $(eqQ)_{OD}=353$ kc/s there results $\alpha^{(Q)}_{3_{13}}=-661$ kc/s and $\alpha^{(Q)}_{2_{20}}=263$ kc/s. Since the $c^{(D)}$ were expected to be quite small, a least squares fit was made directly to the estimated transition frequencies in a manner similar to that used for HDO, and subsequently improved as far as possible.

Frequencies and parameters resulting from this analysis of D_2O are shown in Tables 8 and 9, with the profiles drawn in Figure 4.

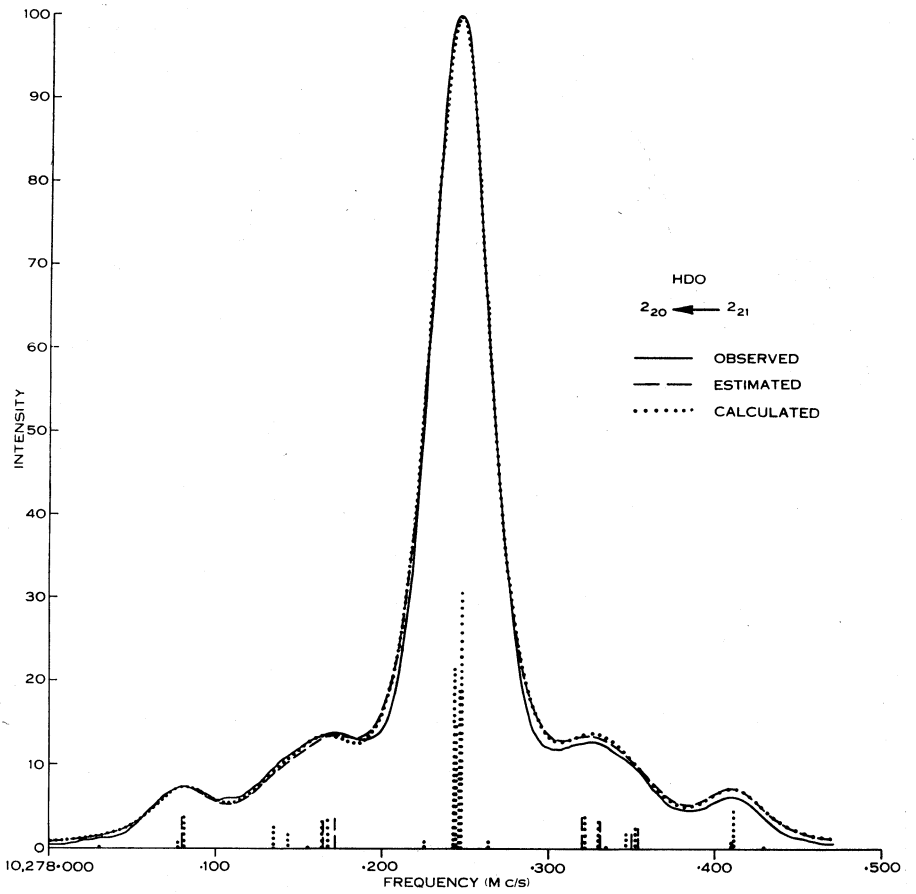

Fig. 1.—Line profiles in the $2_{20}\leftarrow 2_{21}$ transition of HDO. The " estimated " profile was computed using the " estimated " frequencies of Table 7, while the " calculated " profile was obtained using the frequencies computed from final values of the parameters (column (*a*) of Table 9).

IV. Results and Discussion

The major difficulty in the present analysis was to account for the unresolved structure in the HDO spectrum in the region of ± 90 kc/s from the line centre; it can perhaps be regarded as fortunate that agreement could be obtained only for one specific set of values of $c^{(D)}$ and $c^{(H)}$ out of the initial set of 861 trial values.

The magnitude of $c^{(H)}$ ($\sim$240 kc/s) gives rise to frequency shifts of up to 100 kc/s (Fig. 5), which is in the order of that observed in formaldehyde (Okaya 1956). Thus it is apparent that in any molecule in which some or all of the hyperfine

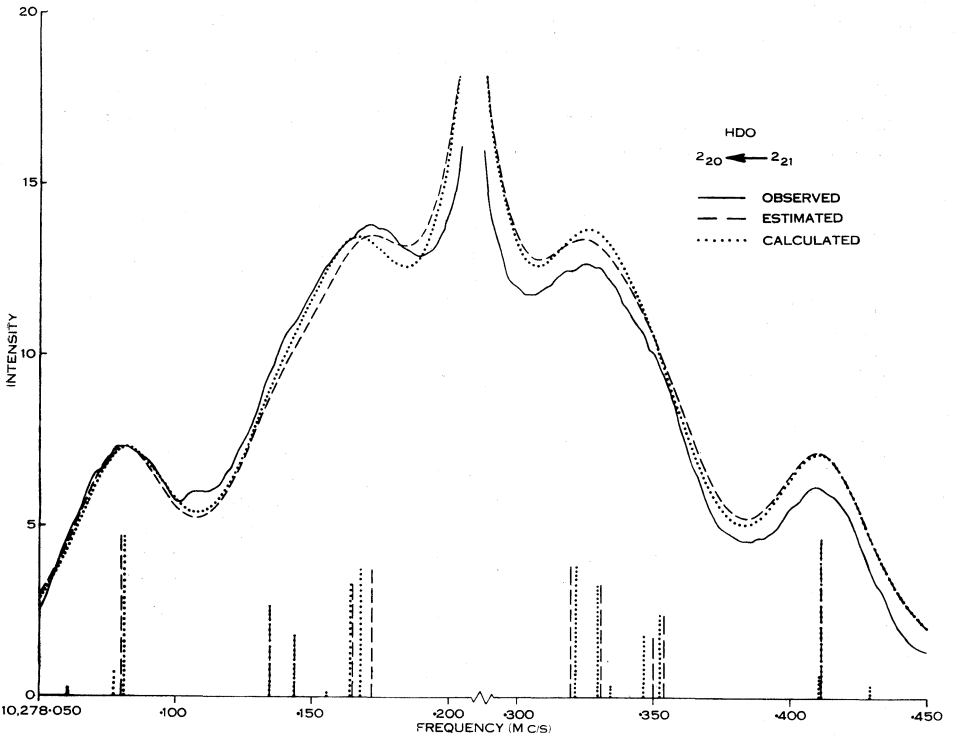

Fig. 2.—Line profiles in the $2_{20} \leftarrow 2_{21}$ transition of HDO. This diagram shows part of Figure 1 with a magnified intensity scale.

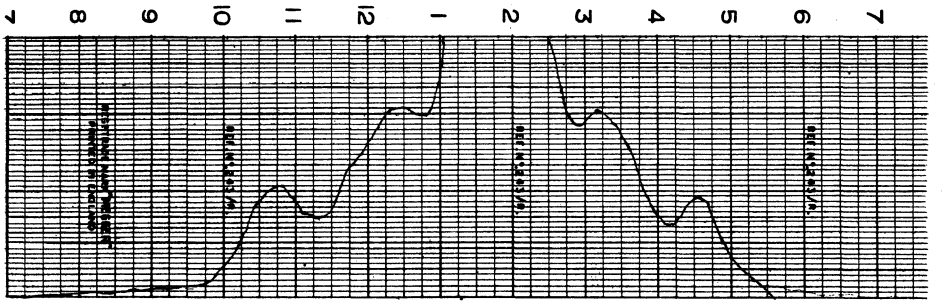

Fig. 3.—High-gain spectrogram of part of the HDO $2_{20} \leftarrow 2_{21}$ transition.

structure is due to both deuterium and hydrogen, both will contribute about equally.

For D_2O the magnetic frequency shifts are much smaller (Fig. 6), and no difficulty was experienced in fitting the spectrum.

The agreement of the final calculated frequencies with the estimated ones to within a few kc/s appears satisfactory. In fact, this agreement is rather better than might have been expected from consideration of the unresolved observations.

TABLE 8

D_2O $3_{13} \leftarrow 2_{20}$ HYPERFINE TRANSITION FREQUENCIES AND RELATIVE INTENSITIES*

		3_{13}					
	I',F' / I,F	2,1	2,2	0,3	2,3	2,4	2,5
2_{20}	2,0	**258±2** 257·7 *12·73*					
	2,1	— 303·9 *12·73*	— 362·1 *25·45*				
	0,2	— 300·9 *0·85*	— 359·2 *8·52*	**300±1** 300·6 *54·23*	— 469·6 *0·04*		
	2,2	— 434·3 *0·97*	— 492·6 *9·67*	— 433·9 *2·38*	**604±1** 603·0 *50·63*		
	2,3		— 470·7 *1·82*	**412±2** 412·0 *6·71*	— 581·1 *12·38*	**521±1** 522·3 *68·18*	
	2,4			— 352·0 *0·32*	— 521·1 *0·59*	**462±2** 462·2 *13·64*	**355±1** 354·2 *100·00*

* The first line of each row shows the estimated frequency (bold type) and the second line shows the frequency calculated from the best D_2O parameters (column (*a*) of Table 9). All frequencies are in kc/s above 10,919·000 Mc/s. The last line of each row gives the relative intensities (italics)

The small r.m.s. errors quoted on the variables are those obtained by applying mechanically the usual theory of random errors (see e.g. Brunt 1931). The possible effects of systematic errors are vividly illustrated in the present problem; in I for D_2O it was assumed that $c^{(D)}=0$, leading to a good least squares fit $(eqQ)_{OD}=+353\pm4$ kc/s (P.E.). The seriousness of the neglect of $c^{(D)}$ and $\alpha^{(S)}$ is shown by the values now obtained of $(eqQ)_{OD}=+315\pm7$ kc/s (r.m.s. error), somewhat outside the previously estimated error limits.

In view of the good fit of calculated and observed profiles it is now profitable to go on to a consideration of the results shown in Tables 8 and 9. In fact, the

relatively large computational effort involved in this analysis was undertaken in the hope that significant results of importance to molecular theory could be obtained, since the possession by nuclei of quadrupole and magnetic moments allows them to act as test probes by means of which we can in principle measure at their geometrical locations the electromagnetic effects of the molecular charge distribution.

TABLE 9
PARAMETERS

	Best Parameters* (*a*) (kc/s)	Calculated Parameters† (*b*) (kc/s)
	HDO	
ν_0	10,278,245·5±1	
$\Delta\nu_0$	21·6	
$\Delta\nu_D$	12·0	
$\Delta\nu_L$	14·2	
$\alpha^{(Q)}_{2_{20}}$	434·4±10	428·3
$\alpha^{(Q)}_{2_{21}}$	419·1±10	424·1
$c^{(D)}_{2_{20}}$	6·7±3	
$c^{(D)}_{2_{21}}$	9·0±3	
$c^{(H)}_{2_{20}}$	242·0±6	
$c^{(H)}_{2_{21}}$	252·0±6	
	D_2O	
ν_0	10,919,422·5±0·6	
$\Delta\nu_0$	18·2	
$\Delta\nu_D$	12·0	
$\Delta\nu_L$	10·0	
$\alpha^{(Q)}_{3_{13}}$	—659·5±7	—660·5
$\alpha^{(Q)}_{2_{20}}$	261·8±3	261·8
$c^{(D)}_{3_{13}}$	42·0±4	
$c^{(D)}_{2_{20}}$	20·1±3	

* The parameters in this column were obtained for each molecule separately.

† The quadrupolar parameters were calculated from the variables shown in Table 10.

(*a*) *Interpretation of the Quadrupole Coupling Constants*

The $\alpha^{(Q)}$ are defined by II, equation (**54**), as linear combinations of $\chi_{gg}=eQ\langle\partial^2V/\partial g^2\rangle$, where the g refer to principal inertial axes of the molecule. Because of Laplace's equation only two of the χ_{gg} are independent. Thus measurements on a single molecule do not completely define the quadrupole coupling tensor,* and it is usual to make some simplifying assumption such as

* Unless certain second-order effects are observable (Kikuchi, Hirota, and Morino 1959).

that the bond direction is a principal axis of this tensor, i.e. that the cross-product terms $\chi_{gg'}$ $(g' \neq g)$ vanish. Sometimes the stronger assumption of cylindrical symmetry about the bond axis is also made (as in I) so that the spectra can be explained in terms of only one quadrupolar coupling constant, that along the bond direction.

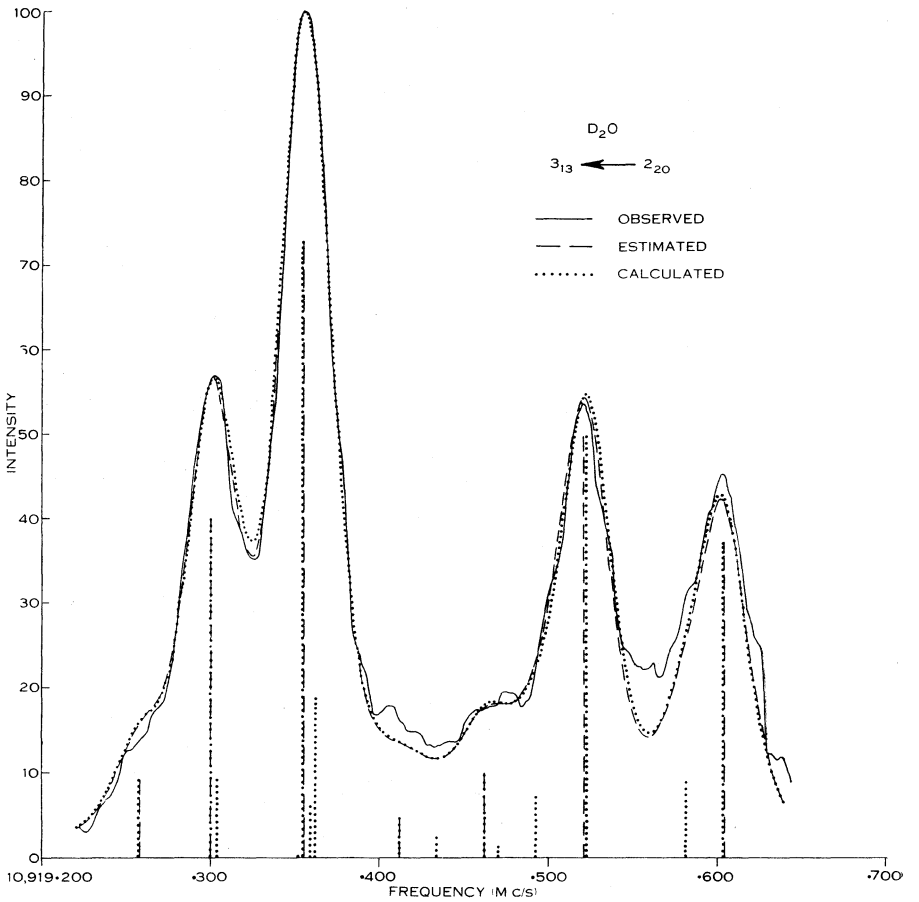

Fig. 4.—Line profiles in the $3_{13} \leftarrow 2_{20}$ transition of D_2O. The " estimated " profile was computed using the " estimated " frequencies of Table 8, while the " calculated " profile was obtained using the frequencies computed from final values of the parameters (column (*a*) of Table 9).

In the present problem we can obtain the χ_{gg} for two isotopic molecules whose principal inertial axes are rotated with respect to one another; the relationship between the two sets of χ_{gg} involves the usually neglected cross-product terms, and thus allows of a complete determination of the tensor. There is, of course, an approximation also involved here, the supposition that the electronic distribution in the two molecules is the same, so giving rise to the same electric field gradient at the deuterons. This is not strictly true, because of the different zero-point vibrations over which the field gradient should be averaged (Newell 1950). However, it is known that in the methyl halides for

example (Simmons and Goldstein 1952), substitution of deuterium for hydrogen changes the observed halogen quadrupole coupling constant by less than 1 per cent., while Newell (1950) has shown that the calculated difference between the electric field gradients in D_2 and in HD is similarly small. Thus it is reasonable to assume that the electric field gradients in HDO and in D_2O will be the same to within about 1 per cent.

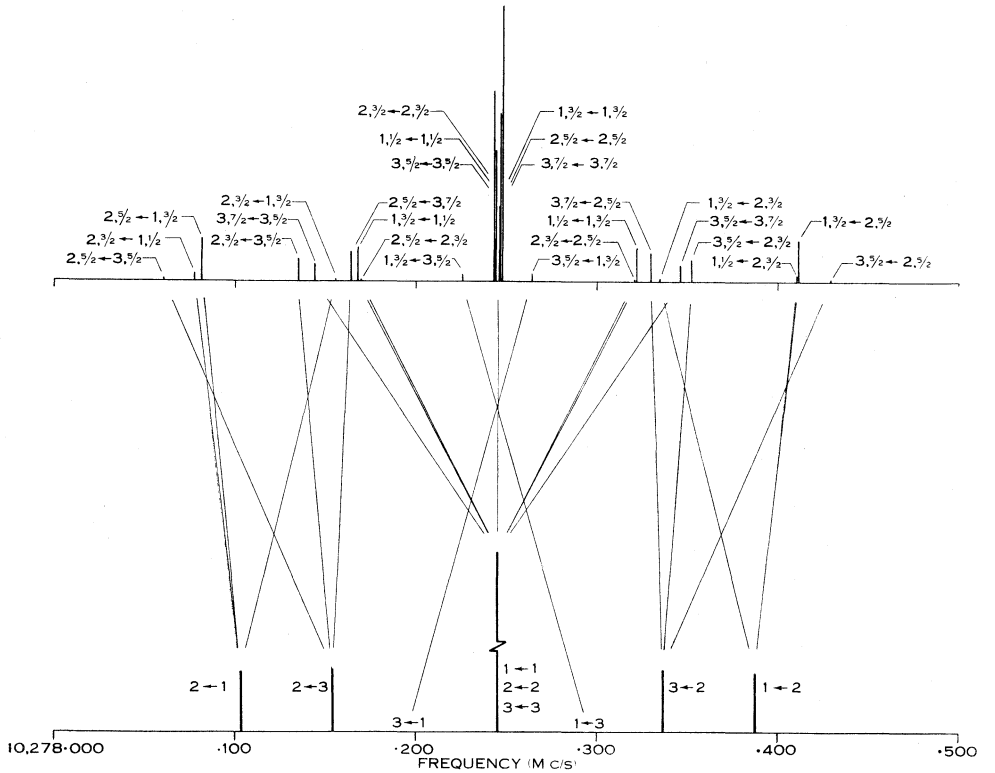

Fig. 5.—Calculated frequencies and relative intensities in the $2_{20}\leftarrow 2_{21}$ transition of HDO. The lower diagram shows the large frequency errors that occur when the magnetic effects are neglected.

If ξ, η, and ζ form a set of right-handed orthogonal axes with the ξ-direction along an OD bond and the η-direction in the molecular plane and pointing towards the bisector of the angle HOH, then, by using standard transformations together with a knowledge of the molecular geometry, we can express the four χ_{gg} (two from each molecule) in terms of three independent variables $\chi_{\xi\xi}$, $\chi_{\xi\eta}$, and $\chi_{\eta\eta}$, which completely specify the quadrupole coupling tensor; we find

$$\left.\begin{aligned}
\alpha^{(Q)}_{2_{20}}(\mathrm{HDO}) &= 1{\cdot}4996\chi_{\xi\xi} - 0{\cdot}7446\chi_{\xi\eta} + 0{\cdot}3658\chi_{\eta\eta},\\
\alpha^{(Q)}_{2_{21}}(\mathrm{HDO}) &= 1{\cdot}3769\chi_{\xi\xi} - 0{\cdot}8233\chi_{\xi\eta} + 0{\cdot}1231\chi_{\eta\eta},\\
\alpha^{(Q)}_{3_{13}}(\mathrm{D_2O}) &= -3{\cdot}6007\chi_{\xi\xi} + 0{\cdot}6060\chi_{\xi\eta} - 3{\cdot}4446\chi_{\eta\eta},\\
\alpha^{(Q)}_{2_{20}}(\mathrm{D_2O}) &= 1{\cdot}1746\chi_{\xi\xi} - 1{\cdot}2343\chi_{\xi\eta} + 0{\cdot}8566\chi_{\eta\eta}.
\end{aligned}\right\} \quad \ldots\ (6)$$

Use of these equations with the $\alpha^{(Q)}$ of column (*a*) in Table 9 then gives the planar components of the quadrupole coupling tensor, as listed in Table 10, and these in

turn give the principal values of this tensor shown in Table 11 ; back-substitution in the equations (**6**) gives the values of the $\alpha^{(Q)}$ shown in column (*b*) of Table 9.

From the accepted value of the quadrupole moment of the deuteron $Q_D=(2\cdot738\pm0\cdot014)\times10^{-27}$ cm^2 (Kolsky *et al.* 1952 ; Quinn *et al.* 1958), the principal values of the electric field gradient at the position of the hydrogen nuclei can be derived. Their magnitudes are also given in Table 11, where comparison is made with quantities computed theoretically by R. Bersohn (1960) from the best available estimate of the electron distribution in the water molecule (Ellison and Shull 1955).

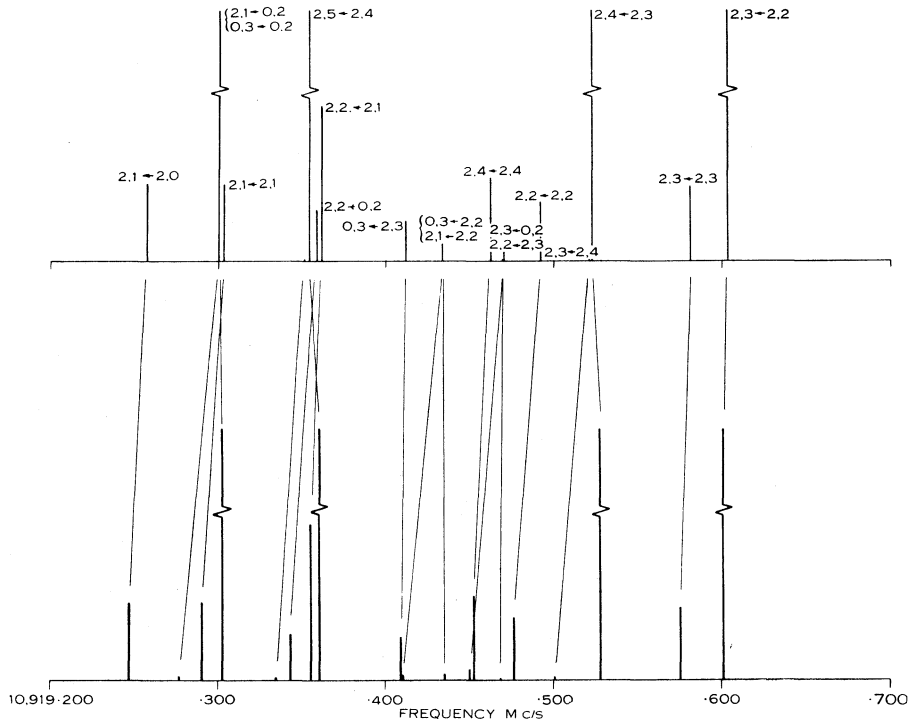

Fig. 6.—Calculated frequencies and relative intensities in the $3_{13}\leftarrow2_{20}$ transition of D_2O. The lower diagram shows that when magnetic effects are neglected small but significant errors occur in calculating the frequencies.

It will be observed that, within the experimental error, the bond direction is in fact a principal axis of the quadrupole coupling tensor in this molecule.

A determination of the electric field gradient in a molecule is usually used to provide some information on the relation of the chemical bond to the nucleus under consideration. In the present case, however, the field gradient arises essentially from the superposition of a number of comparatively small effects, and, without detailed calculation based on better information than is currently available, it is not possible to draw any significant conclusions about the OH bond. The magnitudes of the tensor components, however, give quantitative data which must be accounted for by any complete theory of electron distribution, and to that end they provide a guide for the theoreticians.

(*b*) *Interpretation of the Magnetic Coupling Constants*

The $c^{(k)}$ are also defined by II, equation (**54**), and are linear combinations of the $M_{gg}^{(k)}$ of II, equation (**3**). Partly because the published expression for the $M_{gg}^{(k)}$ is incorrect and partly because of complications in carrying out the required vibrational averaging, it is proposed to discuss the magnetic coupling constants in a later paper.

TABLE 10

QUADRUPOLAR COUPLING TENSOR COMPONENTS

$\chi_{\xi\xi}=eQ_{\mathrm{D}}V_{\xi\xi}=eQ_{\mathrm{D}}(\partial^2V/\partial\xi^2)$	$=315\cdot2\pm7\cdot7$ kc/s
$\chi_{\xi\eta}=eQ_{\mathrm{D}}V_{\xi\eta}=eQ_{\mathrm{D}}(\partial^2V/\partial\xi\partial\eta)=$	$-8\cdot8\pm8\cdot7$ kc/s
$\chi_{\eta\eta}=eQ_{\mathrm{D}}V_{\eta\eta}=eQ_{\mathrm{D}}(\partial^2V/\partial\eta^2)$	$=-139\cdot3\pm7\cdot0$ kc/s

(*c*) *Comparison with Other Work*

Since the completion of the above work Thaddeus and Loubser (1959) have used maser techniques to resolve more completely the hyperfine structure of the HDO transition.* Their experimental results show that the frequencies of lines near 10,278·150 Mc/s and 10,278·350 Mc/s, unresolved here, lie further

TABLE 11

PRINCIPAL VALUES OF THE QUADRUPOLE COUPLING TENSOR AND OF THE ELECTRIC FIELD GRADIENT TENSOR*

Quadrupole Coupling Tensor (kc/s)	Electric Field Gradient Tensor (e.s.u.)	
	Measured	Calculated†
$\chi_{XX}=315\pm7$	$\partial^2V/\partial X^2=1\cdot59\pm0\cdot04\times10^{15}$	$3\cdot27\times10^{15}$
$\chi_{YY}=-140\pm7$	$\partial^2V/\partial Y^2=-0\cdot70\pm0\cdot04\times10^{15}$	$-1\cdot49\times10^{15}$
$\chi_{ZZ}=-175\pm10$	$\partial^2V/\partial Z^2=-0\cdot89\pm0\cdot06\times10^{15}$	$-1\cdot78\times10^{15}$
	$\lvert\eta\rvert=0\cdot115\pm0\cdot061$	$0\cdot092$

* X is rotated 1° 7′±1° 10′ from the ξ-direction towards the bisector of the ∠HOH (calculated† −9·5°).

† Bersohn (1960); Bersohn's x, y, z, and Z correspond to our Z, Y, X, and ξ respectively.

from our assigned values than we had estimated; it is for this reason that the footnote in Section II (*a*) asserts that there is no point to carrying out a recalculation now. However, the overall agreement is very satisfactory since Thaddeus and Loubser find $\alpha^{(Q)}(\mathrm{HDO})=411\cdot1\pm3\cdot2$ kc/s, $(eqQ)_{\mathrm{OD}}=312\cdot5$ kc/s, $|\eta|\leqslant0\cdot15$, $c^{(D)}(\mathrm{HDO})=12\cdot0\pm1\cdot2$ kc/s, and $c^{(H)}(\mathrm{HDO})=259\cdot8\pm2\cdot4$ kc/s, in close agreement

* The D_2O line does not seem to be suitable for this type of experimental investigation (Thaddeus, personal communication).

with the results presented here. When Thaddeus and Loubser's values are used to compute a profile for HDO, we find no better agreement with our experimental results than that previously obtained, indicating that the major source of the discrepancies probably lies in our measurement technique.

The combination of Thaddeus and Loubser's value of $\alpha^{(Q)}$(HDO) with the $\alpha^{(Q)}$'s obtained here for D_2O leads to values for $\chi_{\xi\xi}$ and χ_{XX} of about 305 kc/s.

V. Acknowledgments

The author wishes to thank Mr. W. E. Smith for many valuable discussions and suggestions, and Dr. R. Bersohn, Mr. P. Thaddeus, and Mr. J. Loubser for making available their results prior to publication.

VI. References

Bersohn, R. (1960).—*J. Chem. Phys.* **32**: 85–8.

Brunt, D. (1931).—" The Combination of Observations." (Cambridge Univ. Press.)

Condon, E. U., and Shortley, G. H. (1953).—" The Theory of Atomic Spectra." (Cambridge Univ. Press.)

Ellison, F. O., and Shull, H. (1955).—*J. Chem. Phys.* **23**: 2348–65.

Herzberg, G. (1945).—" Infrared and Raman Spectra of Polyatomic Molecules." (Van Nostrand: New York.)

Kikuchi, Y., Hirota, E., and Morino, Y. (1959).—*J. Chem. Phys.* **31**: 1139–40.

Kolsky, H., Phipps, T. E., Jr., Ramsey, N. F., and Silsbee, H. B. (1952).—*Phys. Rev.* **87**: 395–403.

Newell, G. P. (1950).—*Phys. Rev.* **78**: 711–4.

Okaya, A. (1956).—*J. Phys. Soc. Japan* **11**: 258–63.

Posener, D. W. (1953).—M.I.T. Research Laboratory of Electronics Tech. Rep. No. 255.

Posener, D. W. (1957).—*Aust. J. Phys.* **10**: 276–85.

Posener, D. W. (1958).—*Aust. J. Phys.* **11**: 1–17.

Posener, D. W. (1959).—*Aust. J. Phys.* **12**: 184–96.

Quinn, W. E., Baker, J. M., La Tourrette, J. T., and Ramsey, N. F. (1958).—*Phys. Rev.* **112**: 1929–40.

Simmons, J. W., and Goldstein, J. H. (1952).—*J. Chem. Phys.* **20**: 122–4.

Thaddeus, P., and Loubser, J. (1959).—*Nuovo Cim.* **13**: 1060–4.